IEEE Access
Multidisciplinary | Rapid Review | Open Access Journal

Received February 15, 2020, accepted March 1, 2020, date of publication March 16, 2020, date of current version March 25, 2020.

Digital Object Identifier 10.1109/ACCESS.2020.2980865

Social-Aware D2D Video Delivery Method Based on Mobility Similarity Measurement in 5G Ultra-Dense Network

RUILING ZHANG[1], SHIJIE JIA[1], (Member, IEEE), YOUZHONG MA[1], AND CHANGQIAO XU[2], (Senior Member, IEEE)

[1]Academy of Information Technology, Luoyang Normal University, Luoyang 471934, China
[2]State Key Laboratory of Networking and Switching Technology, Beijing University of Posts and Telecommunications, Beijing 100876, China

Corresponding author: Shijie Jia (shjjia@gmail.com)

This work was supported in part by the Program for Science and Technology Innovation Outstanding Talents in the Henan Province under Grant 184200510011, in part by the Science and Technology Opening Up Cooperation Project of Henan Province under Grant 152106000048, in part by the Science and Technology Key Project of Henan Province under Grant 182102210105, in part by the National Natural Science Foundation of China (NSFC) under Grant 61501216, in part by the Inter-Governmental Science and Technology Cooperation Project under Grant 2016YFE0104600, and in part by the IRTSTHN under Grant 18IRTSTHN014.

ABSTRACT The huge amounts of network traffic generated by the ultra-high-definition video playback of super-large-scale video users results in tremendous pressure for front-haul and back-haul in the 5G network, which brings severely negative influence for the large-scale deployment and scalability of video systems and video delivery performance (e.g. transmission delay and packet loss) related to user quality of experience. The direct D2D communications between mobile devices with adjacent position in geographical area can offloading huge video traffic into the underlying networks, which reduces load of cellular base station in the edge networks and relieves traffic pressure in the core networks. In this paper, we propose a novel Social-Aware D2D Video Delivery Method based on Rapid Sample-Efficient Measurement of Mobility Similarity in 5G Ultra-Dense Network (DMSEM). By investigation for one-hop D2D pair relationship, DMSEM builds a social state transition model of user movement, which makes use of encounter duration and shared video length between encountered users to define the state transition condition. A cluster algorithm of encounter events is proposed, which achieves initial clusters of encounter events by calculating similarity between encounter events from the two aspects of both variation rate of geographical distance between mobile users and encounter duration time. DMSEM makes use of the Fuzzy C-Means to refine the initial clusters and extracts encounter patterns of mobile users. DMSEM designs a sample-efficiency rapid recognition algorithm of encounter pattern, which can use small number of encounter distance samples to achieve fast heuristic recognition of encounter pattern. Extensive tests show how DMSEM achieves better results in comparison with other state-of-the-art solutions in terms of packet loss rate, average freeze time, cache utilization, average bitrate, buffer level and control overhead.

INDEX TERMS Social-aware, video delivery, mobility similarity, 5G ultra-dense network, traffic offloading.

I. INTRODUCTION

The state-of-the-art communication technology 5G not only relies on the expanded bandwidth to support the applications of video services with quality-increasing visual content, but also employs the ultra-dense deployment to provides adequate air interface for the explosive growth of mobile devices in order to deal with the decimated coverage [1]–[7]. The video services with rich visual content and the convenience of ubiquitous access provided by the 5G network attract the vast number of users (The number of video users is 759 million in China until june, 2019). The combination between the super-large-scale users and the high traffic consumption brings tremendous pressure for front-haul and back-haul in the 5G network [8]–[10]. Device-to-Device (D2D) communications enable mobile devices with adjacent position in geographical area to implement direct data transmission without intervention of infrastructure by leveraging licensed cellular

The associate editor coordinating the review of this manuscript and approving it for publication was Ayaz Ahmad.

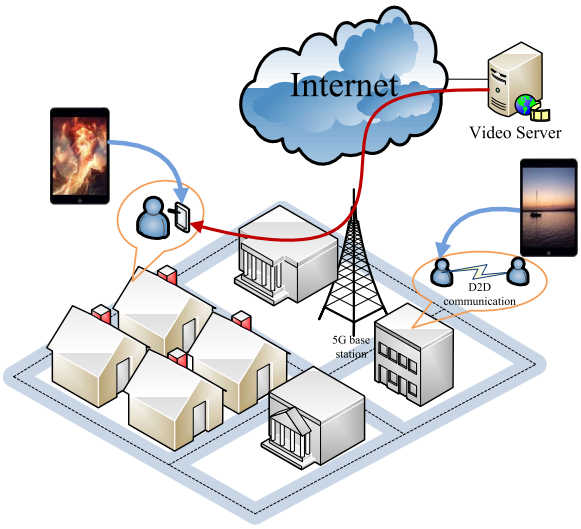

FIGURE 1. Mobile video streaming services in 5G network.

spectrum [11]–[14]. The direct communications between mobile devices can offloading huge video traffic into the underlying networks, which reduces load of cellular base station in the edge networks and relieves traffic pressure in the core networks, as Fig.1 shows. The geographical distance between mobile devices without regard to signal interference is the key factor for performance and efficiency of D2D communications. The stable adjacent distance enables D2D communication pairs to deliver data with low energy consumption and high transmission rate during a relatively long period time. Conversely, the variation of neighbor relationship from one hop to multiple hops brings severely negative influence for performance and efficiency of D2D communications. In fact, the movement behaviors of mobile users have the strong uncertainty. For instance, the sudden change of the weather leads to the immediate adjustments to the original travel schedule. The change of movement behaviors poses a significant challenge to the performance of D2D communications which highly relies on the stability of one-hop neighbor relationship of D2D communicating parties. The accurate pairing of D2D communication parties with long and stable one-hop neighbor relationship is significant for the high-quality video services using the high-efficiency D2D communications.

Sociability is an essential attribute of human movement behaviors [15]. For instance, the employees periodically go there and back at workplace and home and meet with colleagues on workday; the students arrive and depart between school and home and meet with classmate and teachers from Monday to Friday. The sociability of human movement behaviors laies the foundation of content sharing in the edge networks and illustrates appropriate D2D communications pairs [16]- [18]. In other words, the users with long-term frequent encounter and willing content sharing can be considered as the close group such as relatives and friends. The D2D communications between users with close relationship can achieve data exchange with high transmission rate and low energy consumption during a relatively long period time. Numerous researchers focus on improving performance and efficiency of D2D communications by making use of sociability between mobile users. Fan *et al*. make use of social information of interests, behaviors and social tie closeness to measure social relationship levels between mobile users and design a social-aware virtual MAC protocol, which promotes cellular and D2D energy efficiency [19]. Wu *et al*. make use of Jaccard coefficient to measure social similarity between users and design a two-stage social-aware D2D relay selection scheme [20]. Wang *et al*. design a heuristic algorithm of D2D-based content caching and sharing by construction of social propagation in terms of social graphs and user behaviors in online social work and prediction of user mobility [21]. However, the video systems difficultly are aware of classification (e.g. relative and friend) and closeness (e.g. strong and weak) of realistic complex relationship between users. Even if the video systems obtain online social information provided by online social applications, the measurement for social relationship between users in terms of online interaction information difficultly ensures stability and durability of D2D communication pairs. Moreover, except for periodicity, the human movement behaviors also has uncertainty and randomness. For instance, the employees go away on business temporarily on workday instead of going to the office as usual. The uncertainty also bring severely negative influence for stability and durability of D2D communication pairs, which results in interrupt of video data delivery and breaks smoothness of video playback. The stability and durability of D2D communication pairs and uncertainty-tolerant level of movement behaviors are significant for the performance of social-aware D2D-based video sharing and user quality of experience (QoE).

In this paper, we propose a novel Social-Aware D2D Video Delivery Method based on Rapid Sample-Efficient Measurement of Mobility Similarity in 5G Ultra-Dense Network (DMSEM). Our contribution focuses on: 1) the discovery of periodical encounter rule in terms of the sociability of movement behaviors of mobile users and 2) the fast recognition of encounter scenarios suitable for the video sharing using small number of encounter sample data. The detailed contribution is described, as follows.

- We classify the encounter events of mobile users in order to screen out encounter event samples which are fit for one-hop D2D video sharing. Therefore, a social-based state transition model of user movement is proposed, which marks the state of encounter events by comparison between duration time and shared video length in the process of encounter.
- We design a cluster algorithm of encounter events by making use of encounter duration time and variation rate of geographical distance between encounter nodes to express encounter events and map the events into a graph and by iteratively seeks and merges vents mapped in graph in terms of distance between events and centrality gain of mergence.

- We employ the Fuzzy C-Means (FCM) to remove noises in initial event cluster and refine accuracy levels of initial clustering because the low accuracy of clustering encounter events brings negative influence for the accurate recognition of movement behaviors of mobile users.
- We further extracts encounter patterns of mobile users from the refined event clusters and design a sample-efficiency rapid recognition algorithm of encounter pattern, which can use small number of encounter distance samples to achieve fast heuristic recognition of encounter pattern.
- Extensive tests show how DMSEM achieves better results in comparison with other state of the art solutions in terms of packet loss rate, average freeze time, cache utilization, average bitrate, buffer level and control overhead.

II. RELATED WORK

Recently, numerous researchers focus on leveraging social relationship between mobile devices to promote performance of D2D communication with low energy consumption. Ying *et al*. proposed a social-aware relay selection method for multi-hop D2D communications (PSRS) [22]. PSRS measures closeness of social relationship between mobile users in terms of interaction and contribution and estimates transmission consumption in terms of D2D communication distance. PSRS formulates and solves an optimal relay selection problem based on constraints of social relationship and transmission consumption in the process of multi-hop D2D communication path selection, which efficiently enhances performance of multi-hop D2D communications. Fan *et al*. designed a social-aware virtual MAC protocol by integrating virtualization and social-awareness features for D2D communications [19]. By gathering social information of users, the mobile devices can efficiently search potential D2D pairs and associates D2D objective devices. In order to promote efficiency of cellular and D2D resource allocation, the two optimization problems are proposed: 1) the optimization problem of cellular resource allocation; 2) The optimization problem of D2D resource allocation. By solving the above two optimization problems, a joint D2D channel-power allocation method is proposed, which achieves energy efficiency of D2D and cellular resource allocation.

Wu *et al*. formulated a multi-objective binary integer linear programming problem for social-aware D2D user-equipment-to-network relay selection [20]. A joint decision weight generation strategy by incorporating both subjective and objective preferences is proposed, which estimates the relative proximity degree of relay helper of user equipment from the perspective of victim user equipment. The optimal solution corresponding to the formulated problem is obtained in terms of the relative proximity degree. The user-centric social-aware D2D relay selection algorithm is design, which promotes network capacity and improves accessability of user equipment. Zhao *et al*. considered the integration between social relationships based on the complex social connections in the continuum space and the resource allocation for D2D communications [23]. By formulating a social group utility maximization game with the purpose of maximization of social group utility of each D2D user, the joint performance of social and physical domains can be quantitatively measured. The distributed algorithm of resource allocation based on the switch operations is proposed in terms of theoretical investigation for the Nash Equilibrium of the game. Zhang *et al*. proposed a social-aware peer discovery strategy for D2D communication underlaying cellular networks [40]. By investigation for contact rates and centralities of users, the users are divided into multiple communities in terms of the community detection algorithm K-CLIQUE. D2D pair probe with constant intervals can obtain an acceptable performance, which is better than other probe strategies. Further, the maximization problem of number of effective contacts with energy budget constraints is formulated and solved, which optimizes the detection of potential D2D pairs and reduces energy consumption. Chen *et al*. proposed a social-aware cooperative device-to-device (D2D) communication method [25]. The physical constraints for feasible D2D cooperation is modeled in terms of the physical graphs; The social trust among the nodes is modeled in terms of the social graphs. A network-assisted relay selection mechanism is designed, which supports implementing the coalitional game solution to promote efficiency of D2D cooperation. Chen *et al*. proposed a social-trust-aided D2D communication framework by making use of the social trust to promote performance of D2D communication [26]. The clustering coefficient in graph theory is used to define social-link probability, namely social trust among cellular and D2D users. By utilizing stochastic geometry to quantitatively analyze the social trust rate for D2D communications, the theoretical bound of potential performance gains using social trust among mobile users with secure transmission is obtained. An optimization problem of resource allocation for maximizing the system social trust rate is formulated. The implementation mechanism of resource allocation among multiple users in terms of the matching theory is designed, which promotes security and performance of D2D communications. However, the above methods only consider social relationship to implement D2D communications. Because the closeness degree of social relationship does not ensure stability and durability of D2D communication distance between mobile devices, the dynamic movement behaviors of mobile devices brings severely negative influence for the performance D2D communications of the above methods.

The dynamic mobility between D2D communication pairs is the main reason for influencing performance of D2D-based content delivery. Leveraging mobility measurement of mobile devices to ensure stability of geographical distance between them becomes an important method of promoting content sharing performance in the edge network. Yoon *et al*. built a mobility model of mobile users based on the realistic movement traces [27]. The movement trajectories of mobile users is defined as the set of network infrastructure (e.g. WiFi and APs) accessed by the mobile users. By collecting the original movement trajectories of mobile nodes in an actual map,

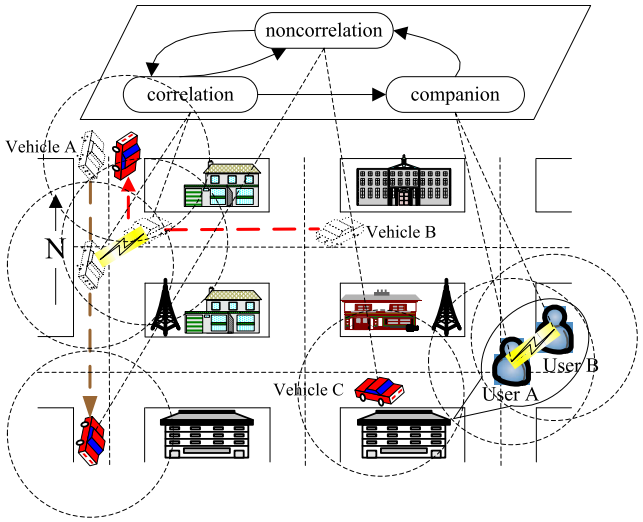

FIGURE 2. Social-based state transition of user mobility.

the original movement trajectories are refined and the refined trajectories further are converted to a graph of mobility of mobile users. Based on the built graph, the movement patterns of mobile users are extracted by calculating frequency of the mobile users passing the APs and the probability of the mobile users passing the APs in the future can be calculated. Waqas *et al*. investigated the adoption and implementation of D2D communication technology from the mobility aspects of D2D communication [28]. The state-of-the-art problems and the corresponding solutions for encouraging the exploitation of mobility to assist D2D communications is extensively reviewed. The advantages and existing problems of mobility-aware D2D communication are summarized and the open issues and future research directions concerning D2D communication applications in real-life scenarios are discussed.

III. DMSEM DETAILED DESIGN

A. SOCIAL-BASED USER MOVEMENT STATE

The D2D communications allow direct delivery of video data between nodes without the intervention of cellular tower, which reduces data forwarding load of cellular tower and enhances performance of data transmission. The D2D participators need to enable the geographical distance between them always be less than the radius of their communication range and have slight fluctuation, namely there is a stable one-hop neighbor relationship with each other during a long period time. The change of geographical location caused by mobility of mobile users is main reason which leads to the change of one-hop relationship (from one-hop to multiple hops). However, the mobility of mobile users also has periodicity and pseudo-randomness because of human sociality, so that the stability of one-hope relationship between participant D2D nodes can be estimated and predicted.

As Fig.2 shows, the movement behaviors between mobile users have the three states: 1) Noncorrelation: When the geographical distance between the two nodes is larger than their communication radius (e.g. vehicle A and C), their states are considered as the noncorrelation; 2) Correlation: the geographical distance between the two nodes is less than their communication radius and they keep the one-hop neighbor relationship during a short period time (e.g. encounter of vehicle A and B at road intersection), their states are considered as the correlation; 3) Companion: When the two nodes keep the one-hop neighbor relationship during a long period time, their states are considered as the companion because the long-term one-hop relationship provides enough delivery time of video data (e.g. user A and B). There is transition among the three states due to the dynamic movement behavior of users:

1) Noncorrelation → Correlation: When the two nodes have multihop relationship at t_i, respectively and they become one-hop neighbor at t_{i+1}, their states make a transition from noncorrelation to correlation. For instance, when the two vehicles A and B drive from different area to encountered road intersection and become one-hop neighbors, their states change from noncorrelation to correlation.

2) Correlation → Noncorrelation: When the two nodes keep one-hop neighbor relationship during a short period time Δt and become multihop relationship after Δt, their states change from correlation to noncorrelation. For instance, the two vehicles A and B drive from the short-term encounter at road intersection to running in the opposite direction.

3) Correlation → Companion: When the two nodes keep one-hop relationship from a short period time to a long period time, their states change from correlation to companion. For instance, the two users A and B encounter in the building and keep encounter state during a long period time;

4) Companion → Noncorrelation: When the two nodes which have a long-term one-hop neighbor relationship become multihop relationship, their states change from companion to noncorrelation.

The ''correlation'' and ''companion'' state rely on the common precondition: the one-hop neighbor relationship between the two mobile nodes; The difference between ''correlation'' and ''companion'' state focuses on duration time of one-hop neighbor relationship. Because the encounter time of the two mobile nodes is unidirectional increasing, the ''companion'' state is not changed into the ''correlation'' state. Once the two mobile nodes which keep the ''correlation'' state lose their one-hop neighbor relationship, their ''correlation'' state is changed into the ''noncorrelation'' state.

The distinct transition conditions from noncorrelation/correlation to correlation/noncorrelation and from companion to noncorrelation denote the variation from one-hop/multihop to multihop/one-hop. However, the transition condition from correlation to companion is based on the indistinct description for the boundary between short and long period time of one-hop relationship. We need to further clearly define the transition condition from correlation to companion. The long-term one-hop relationship can avoid severe fluctuation of video data transmission performance caused by the variation from one-hop to multihop, so the low

transmission delay and packet loss rate of one-hop D2D communications can meet the demand of delay-sensitive video services. If the time length of one-hop relationship between nodes is equal or greater than the time length required by transmission of video data, the encounter state of nodes can be considered as the companion. For instance, a mobile node n_i has m one-hop neighbors $N_i = (n_1, n_2, \ldots, n_m)$. n_i is a receiver and n_i's SINR (Signal to Interference plus Noise Ratio) corresponding to any node n_j in N_i can be defined as $\gamma_{j,i}$ [29]. The larger the value of $\gamma_{j,i}$ is, the easier the matching level between n_i and n_j is. The received and sent power and geographical distance in $\gamma_{j,i}$ are the two important impact factors for the successful pairing between adjacent devices. If the geographical distance between n_i and n_j is long, n_i and n_j need to increase their received and sent power in order to avoid fast signal fading and achieve successful matching; Otherwise, if the geographical distance between n_i and n_j is short, n_i and n_j can keep the low-level power to achieve successful matching. The close and stable geographical distance between n_i and n_j not only reduces power consumption, but also decreases risk of matching failure.

After the successful matching, n_i and n_j transmit data with each other. In terms of the Shannon formula [30], the link rate between n_i and n_j can be defined as $R_{j,i} = B_{j,i}\log_2(1 + \gamma_{j,i})$, where $B_{j,i}$ is the communication bandwidth between n_i and n_j. The $\gamma_{j,i}$ and bandwidth $B_{j,i}$ between n_i and n_j are key factors for the values of $R_{j,i}$. If the value of $B_{j,i}$ is a constant or keeps very slight fluctuation in the small range, the value of $R_{j,i}$ keeps the increase trend with increasing value of $\gamma_{j,i}$. The stable and close geographical distance between n_i and n_j reduces the sent and received power and the signal fading level, which enables the value of $\gamma_{j,i}$ to keep the high levels. Therefore, when the value of $\gamma_{j,i}$ keeps the high levels, the high-level value of $R_{j,i}$ ensures the fast transmission of video data between n_i and n_j, which reduces the transmission time. The D2D participators usually employ the periodical search strategy of D2D communication object, which increases the probability of matching D2D communication object. Let T denote the period time of searching one-hop D2D communication object. If n_j is the one-hop neighbor of n_i between k^{th} search period of n_i, the gain of one-hop neighbor relationship between n_j and n_i can be defined as:

$$G_{j,i}^k = w_{j,i}^k S_{j,i}^k \tag{1}$$

where $S_{j,i}^k$ denotes the size of video data which can be transmitted between n_j and n_i during the period time $T_{j,i}$; $S_{j,i}^k = P_{j,i}^k R_{j,i}^k T_{j,i}^k$ where $P_{j,i}^k$ is the frame loss rate of current channel during k^{th} search period; $R_{j,i}^k$ is the link rate between n_j and n_i during k^{th} search period; The higher the link rate $R_{j,i}$ is, the more the gain $G_{j,i}$ of one-hop neighbor relationship between n_j and n_i is. $T_{j,i}^k \in (0, T]$ is the time length of one-hop neighbor relationship of n_j and n_i during k^{th} search period; $w_{j,i}^k$ is a social factor for the gain of encounter between n_j and n_i and is defined as:

$$w_{j,i}^k = \frac{F_{j,i}}{\sum_{c=1}^{m} F_{c,i}}, w_{j,i}^k \in [0, 1] \tag{2}$$

where $F_{j,i}$ is the total number of encounter between n_j and n_i; m is the total number of encountered one-hop neighbor nodes of n_i; $\sum_{c=1}^{m} F_{c,i}$ denotes the total number of encounter between n_i and m one-hop neighbor nodes. $w_{j,i}$ can be considered as the credibility level of stability of one-hop neighbor relationship between n_j and n_i. If there is the frequent encounter between n_j and n_i, the one-hop neighbor relationship between them is reliable and their encounter can be considered as the recurrent event; If there is the infrequent encounter between n_j and n_i, the one-hop neighbor relationship between them is unreliable and fragile and their encounter can be considered as the accidental event. The frequent encounter between n_j and n_i enables the value of $w_{j,i}$ increase and further promote the gain $G_{j,i}$.

When n_j and n_i continuously encounter and the cumulative time of encounter between n_j and n_i can support the long-term video sharing with one-hop neighbor relationship, the ''correlation'' state between n_j and n_i can be changed into the ''companion'' state. If n_j still has the one-hop neighbor relationship with n_i after experiencing h period of n_i, the cumulative sum of gain of one-hop neighbor relationship between n_j and n_i is $\sum_{c=1}^{h} G_{j,i}^c$. If $\sum_{c=1}^{h} G_{j,i}^c \geq \bar{S}$, the state of n_j and n_i occurs to change from correlation to companion where $\bar{S} = \frac{\sum_{c=1}^{k} S_{c,i}}{k}$. k is the total number of all one-hop neighbor nodes which have shared videos with n_i. Because the video resource sharing is not necessary after each encounter of the two mobile nodes, the value of k (the total number of video sharing of n_i) may be equal or unequal to m (the total number of encountered one-hop neighbor nodes of n_i); $S_{c,i}$ is the size of shared video data between any one-hop neighbor n_c and n_i; The size of each shared video can be computed in terms of the length and playback rate of shared video files. $\bar{S}$ is average size of shared video files between n_i and historical all one-hop neighbor nodes. $\sum_{c=1}^{h} G_{j,i}^c \geq \bar{S}$ means that the encounter duration time of n_j and n_i (the movement behaviors of n_j and n_i has enough stability) can support delivery of the whole video data.

B. CHARACTERISTIC EXTRACTION OF ENCOUNTER EVENT

The encounter among the mobile nodes can be considered as the event. In fact, the encounter among the mobile nodes is caused by the event in real life. For instance, the vehicles in the process of driving accidentally encounter in a road intersection or a road. This is because the travel planning formulated by the drivers includes the same road intersection or road in advance. The two users periodically encounter in the office because of their colleague relationship. However, the video system difficultly fetches the complex social

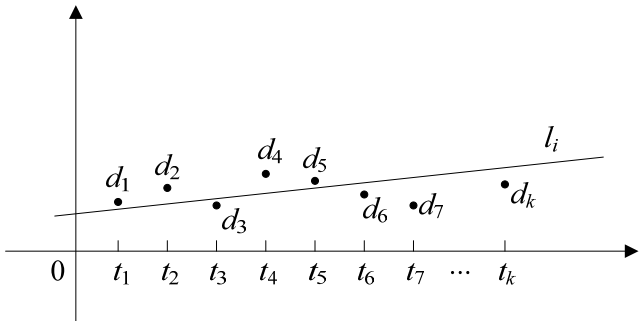

FIGURE 3. Distribution of geographical distance between n_j and n_i with increasing timestamp.

knowledge to recognize what kind of event happens. In other words, the video system only is aware of mobility level and encounter time length of nodes in the encounter events. Therefore, the duration length and mobility level can be used to describe the encounter event. When the encounter event occurs, the video system can recognize what kind of encounter event happens in terms of the matching level of event characteristics.

Based on the above mentioned state transition condition from correlation to companion, the events corresponding to the companion state of n_j and n_i form a set $E_{j,i} = (e_1, e_2, \ldots, e_n)$. We only focus on the event corresponding to the companion state of n_j and n_i because the companion event can support the delivery of the whole video data. Any item e_i in $E_{j,i}$ can be defined as $e_i = (l_i, b_i)$. L_i is the duration length of e_i and the value of L_i can be defined as the difference between the ending and beginning time of encounter; b_i denotes the variation rate of geographical distance between n_j and n_i. The variation of geographical distance between nodes brings severely negative influence, so the variation rate of geographical distance is the important factor for the stability of one-hop neighbor relationship between encountered nodes. For instance, the increase in the geographical distance between nodes results in the greater attenuation of channel signal, which reduces the matching success ratio of D2D participators and decreases the transmission rate of video data. n_i periodically searches the D2D communication objects in e_i, namely the duration length of e_i is consisted of several search period. n_i can obtain the geographical distance between n_i and n_j after experiencing each search period by exchange of geographical location information. The values of geographical distance between n_j and n_i after experiencing each search period form a set $DS_{j,i}(t) = (d_1(t_1), d_2(t_2), \ldots, d_k(t_k))$ where t is the timestamp of search period of n_i. All items in $DS_{j,i}$ keep discrete distribution in a two-dimensional surface with linear increase of timestamp. As Fig.3 shows, the abscissa and ordinate in the two-dimensional surface denote timestamp and geographical distance, respectively. The variation of geographical distance can reflect the stability of one-hop relationship between n_j and n_i. We employ the slope $b_{j,i}$ of linear regression fitting line for all items in $DS_{j,i}$ to denote the variation rate of geographical distance between n_j and n_i with increasing time by making use of the least square method [31]–[33].

$$b_{j,i} = \frac{\sum_{c=1}^{k} t_c d_c - k\bar{t}\bar{d}}{\sum_{c=1}^{k} t_c^2 - k\bar{t}^2} \tag{3}$$

where $\bar{t}$ and $\bar{d}$ denote the mean values of time length and geographical distance in $DS_{j,i}$, respectively. $b_{j,i} > 0$ denotes that the geographical distance keeps increasing trend; Otherwise, $b_{j,i} < 0$ denotes that the geographical distance keeps decreasing trend. If the value of $|b_{j,i}|$ ($b_{j,i}$'s absolute value) keeps relatively high level, the variation level of geographical distance between n_j and n_i is high. Similarly, the values of b in other events can be defined according to $b_{j,i}$.

n_i encounters with many nodes in the process of movement, which generates a large amount of encounter events corresponding to n_i and n_i's encountered nodes, namely the events form a set E_i. In fact, there are the frequent encounter events with the same characteristics in E_i. For instance, the encounter between colleagues on weekdays can be considered as the periodical frequent events. The events which have similar duration length and variation rate of mobility can be considered as the same kind of events. Therefore, by clustering all items in E_i in terms of similarity of duration length and variation rate of mobility, E_i can be expressed by a small number of representative events. Because any item in E_i is denoted by duration length l and mobility variation rate b, all items in E_i can be mapped in a two-dimensional surface where the abscissa and ordinate in the two-dimensional surface denote duration length and mobility variation rate, respectively. Each item e_x in E_i can obtain the Euclidean distance from e_x to other items in E_i according to the following equation [34].

$$d_{x,y} = \sqrt{(l_x - l_y)^2 - (b_x - b_y)^2} \tag{4}$$

where l_x and l_y are the duration length of encounter between e_x and e_y, respectively; b_x and b_y are the variation rate of geographical distance between e_x and e_y, respectively. The Euclidean distance between e_x and other items in E_i form a set $DS_x = (d_{1,x}, d_{2,x}, \ldots, d_{n,x})$.

C. CONSTRUCTION OF INITIAL ENCOUNTER EVENT CLUSTER

Each item in E_i calculates the Euclidean distance with other items in E_i. In terms of the Euclidean distance between items in E_i, the centrality of any item e_x can be defined as [35]:

$$C_x = \frac{\sum_{c=1}^{|E_i - e_x|} d_{c,x}}{|E_i - e_x|} \tag{5}$$

where $d_{c,x}$ denotes the Euclidean distance between e_x and any item e_c in E_i; $|E_i - e_x|$ returns the number of items in the difference set between E_i and e_x. $\sum_{c=1}^{|E_i - e_x|} d_{c,x}$ is the

cumulative sum of Euclidean distance between e_x and other $n-1$ items in E_i. C_x is the centrality of e_x corresponding to $n-1$ items in E_i. Similarly, other $n-1$ items in E_i can obtain their set of Euclidean distance and the centrality values. Each item in E_i is discretely distributed in the two-dimensional surface and initially is considered as a cluster. For instance, the cluster consisted by e_x can be expressed as $S_x = (e_x)$. In fact, clustering discrete data into multiple sets can be considered as the process of discovery of data which has close Euclidean distance. In other words, the clusters in DS_x focus on the mergence with data which has the shortest Euclidean distance. The mergence process can be described in terms of the following steps.

Step 1: Initially, each cluster in E_i only contains an event and needs to search the event which has the shortest Euclidean distance. For instance, S_x only contains e_x and e_x can obtain a subset $DS_x^{(1)}$ ($DS_x^{(1)} \in DS_x$) where all items in $DS_x^{(1)}$ have the shortest Euclidean distance with e_x. If e_x merges any item e_y in $DS_x^{(1)}$, the centrality gain of e_x can be defined as:

$$MG_x = C_x^{(1)} - C_x, C_x^{(1)} = \frac{\sum_{c=1}^{|E_i - e_x - e_y|} d_{c,x}}{|E_i - e_x - e_y|} \tag{6}$$

where $|E_i - e_x - e_y|$ returns the number of items in the difference set among E_i, e_x and e_y. $C_x^{(1)}$ is the centrality of e_x after e_x removes the connection with e_y. MG_x denotes the increment of centrality of e_x before and after e_x removes the connection with e_y. $MG_y = C_y^{(1)} - C_y$ is the centrality gain of e_y after the mergence. $C_y^{(1)}$ is the centrality of e_y after e_y removes the connection with e_x. Let $S_x^{(1)}$ denote a cluster built by e_x and e_y and the mergence gain of e_x and e_y can be defined as:

$$MG_{x,y} = \sum_{c=1}^{|S_x^{(1)}|} MG_c \tag{7}$$

where $|S_x^{(1)}|$ returns the number of items in $S_x^{(1)}$ after the mergence, namely $S_x^{(1)} = (e_x, e_y)$. $MG_{x,y}$ denotes the total number of centrality increment of all items in $S_x^{(1)}$ after the mergence. In terms of the above process, e_x calculates the gain values by merging each item in $DS_x^{(1)}$.

Similarly, other $n-1$ items in E_i also calculate their mergence gains with the events which have the shortest Euclidean distance with them. The gain values of all items in E_i form a set $GS_i = (MG_{1,2}, MG_{1,3}, \ldots, MG_{m,n})$. Each item in GS_i is corresponding to a new merged cluster among all items in E_i. However, the merged results should meet the requirement: the intersection between clusters is empty. Therefore, the redundancy items in GS_i can be removed from GS_i. The process of cluster mergence is described, as follows.

(1) Let MG_{max} denote the largest value among all items in GS_i. The merged cluster corresponding to the largest value MG_{max} is defined as: S_{max}.

(2) If the merged clusters corresponding to all items in GS_i includes any event in S_{max}, the gain values corresponding to these clusters are removed from GS_i. The remaining items in GS_i form a new set $GS_i^{(1)}$.

(3) Let $GS_i = GS_i^{(1)}$ and return (1).

The convergence condition of the above iterative mergence is that GS_i becomes an empty set. After the mergence iteration, the merged clusters form a new set CS_i.

Step 2: Each cluster in CS_i attempts to search and merge new events included in other clusters. The events included in each cluster in CS_i select the events which have the shortest Euclidean distance with them as the object to be merged. For instance, a cluster $S_x^{(1)} = (e_x, e_y)$ in CS_i includes the two events e_x and e_y. The event sets which have the shortest Euclidean distance with e_x and e_y are defined as $DS_x^{(2)}$ and $DS_y^{(2)}$, respectively where $e_y \notin DS_x^{(2)}$ and $e_x \notin DS_y^{(2)}$. If an Euclidean distance between e_x and any item in $DS_x^{(2)}$ is less than that between e_y and any item in $DS_y^{(2)}$, all items in $DS_x^{(2)}$ can be considered as the object to be merged; Otherwise, If an Euclidean distance between e_x and any item in $DS_x^{(2)}$ is larger than that between e_y and any item in $DS_y^{(2)}$, all items in $DS_y^{(2)}$ can be considered as the object to be merged; If the Euclidean distance between e_x and any item in $DS_x^{(2)}$ is equal to that between e_y and any item in $DS_y^{(2)}$, all items in $DS_x^{(2)} \cup DS_y^{(2)}$ can be considered as the object to be merged. Let e_h be an item in the merged objects and $C_x^{(1)}$ is the centrality of e_x staying in $S_x^{(1)}$.

$$C_x^{(1)} = \frac{\sum_{c=1}^{|E_i - S_x^{(1)}|} d_{c,x}}{|E_i - S_x^{(1)}|} \tag{8}$$

where $|E_i - S_x^{(1)}|$ returns the number of items in the difference set between E_i and $S_x^{(1)}$. Let $C_x^{(2)}$ be the centrality of e_x after e_h is merged into $S_x^{(1)}$.

$$C_x^{(2)} = \frac{\sum_{c=1}^{|E_i - S_x^{(1)} - e_h|} d_{c,x}}{|E_i - S_x^{(1)} - e_h|} \tag{9}$$

If e_h is merged into $S_x^{(1)}$, the centrality gain of e_x can be defined as $MG_x = C_x^{(2)} - C_x^{(1)}$. Similarly, if e_h is merged into $S_x^{(1)}$, e_y also has the centrality gain MG_y. Let $C_h^{(1)}$ be the centrality of e_h staying in the current $S_h^{(1)}$, $e_h \in S_h^{(1)}$. Let $C_h^{(2)}$ denote the centrality of e_h after e_h join into $S_x^{(1)}$ and $C_h^{(2)}$ can be defined as:

$$C_h^{(2)} = \frac{\sum_{c=1}^{|E_i - S_x^{(1)} - e_h|} d_{c,h}}{|E_i - S_x^{(1)} - e_h|} \tag{10}$$

$MG_h = C_h^{(2)} - C_h^{(1)}$ is the centrality gain of e_h after e_h join into $S_x^{(1)}$. If e_h joins into $S_x^{(1)}$, e_x, e_y and e_h form a new cluster $S_x^{(2)}$. $MG_{x,y,h} = \sum_{c=1}^{|S_x^{(2)}|} MG_c$ is the mergence gain of all items in $S_x^{(2)}$.

Algorithm 1 Construction of Initial Event Cluster

/*$CS_i^{(m)}$ is cluster set of n_i at m^{th} round; */
$m = 1; n = 2;$
each event in E_i is a cluster and is added into CS_i;
calculates centrality of events in $CS_i^{(m)}$ by eq.(7);
while$(CS_i^{(m)} != CS_i^{(n)})$
  $CS_i^{(m)} = CS_i^{(n)}$; $CS_i^{(n)} =$ Null;
  for$(h = 0; h < |CS_i|; h{+}{+})$
    for$(j = 0; j < |CS_i|; j{+}{+})$
      if $(h != j)$
        calculates distance d between $CS_i[h]$ and $CS_i[j]$;
        d_h is added into list DS_h;
      end if
    end for
    Extracts minimum distance set $DS_h^{(1)}$ from DS_h;
    combinational set of $CS_i[h]$ and items $DS_h^{(1)}$ is MS_h;
    for$(j = 0; j < |MS_h|; j{+}{+})$
      calculates gain of $MS_h[j]$ by eq.(9);
      $MG_{h,j}$ is added into list GS_h;
    end for
    while$(|MS_h| != 0)$
      selects item MG_{max} with largest value from MS_h;
      S_{max} is combination corresponding to MG_{max};
      S_{max} is added into set $CS_i^{(n)}$;
      for$(j = 0; j < |S_{max}|; j{+}{+})$
        MS_h removes item which includes event $S_{max}[j]$;
      end for
    end while
  end for
  $m{+}{+}; n{+}{+};$
end while

In terms of the above method, the mergence gains of $S_x^{(1)}$ merging other objects can be obtained. Similarly, the mergence gains generated by all clusters in CS_i merging their merged objects also are calculated. All mergence gains can form a new set $GS_i = (MG_{1,2}, MG_{1,3}, \ldots, MG_{m,n})$. Each item in GS_i is corresponding to a new merged cluster among all items in E_i. In order to ensure the intersection between the merged clusters be empty, the redundancy items in GS_i can be removed from GS_i in terms of the process of Step 1.

Step 3: In terms of the process of cluster mergence in Step 1 and 2, the events in clusters of $CS_i^{(2)}$ continue to search the merged objects which have the shortest Euclidean distance with them. The continuous cluster mergence results in increase in the number of events in clusters, so that the similar events are merged into the same cluster. The convergence condition of cluster mergence can be defined as: all clusters in $CS_i^{(n)}$ (the generated cluster set after the n^{th} round mergence) cannot merge any event in other clusters, namely $CS_i^{(n)} = CS_i^{(n+1)}$. At the moment, $CS_i^{(n)}$ includes the initial event clusters. Algorithm 1 describes the construction process of initial event cluster.

D. CONSTRUCTION OF ENCOUNTER EVENT PATTERN

The centrality of any event is considered as the relative location represented by other $n-1$ events. The construction of initial event clusters in $CS_i^{(n)}$ relies on high centrality gains generated by the events with high centrality to adsorb the events which has low centrality. The events with high centrality may assimilate the events which have more far distance with them into current clusters, namely the initial event clusters in $CS_i^{(n)}$ may include some noise events. The noise events bring severely negative influence for the representation accuracy of encounter patterns. Therefore, we make use of the Fuzzy C-Means (FCM) to remove noises and refine accuracy levels of clustering events [36].

Because all items in $CS_i^{(n)}$ are acentric clusters, the centric nodes should be selected from each item in $CS_i^{(n)}$. For instance, any cluster $S_x \in CS_i^{(n)}$ includes the events $e_x, e_y, \ldots, e_h$. The average value of distance between any event e_x and other events in S_x can be defined as:

$$\bar{d}_x = \frac{\sum_{c \neq x, c \in S_x} d_{c,x}}{|S_x| - 1} \tag{11}$$

where $|S_x|$ returns the number of items in S_x. Similarly, the average distance values of other items in S_x can be calculated. If an item in S_x has the least value among average distance values of all items in S_x, the item is considered as centric node of S_x; If there are multiple items with the least value in S_x, the item which has the least centrality is considered as centric node of S_x. In terms of the above process of selection of centric node in S_x, the centric nodes of other clusters in $CS_i^{(n)}$ also can be selected. The membership of any item e_y corresponding to S_x in $CS_i^{(n)}$ can be defined as [36]:

$$M_{y,x} = \sum_{c=1}^{|CS_i^{(n)}|} \left(\frac{d_{y,x}}{d_{c,x}}\right)^{\frac{2}{m-1}}, M_{y,x} > 0 \tag{12}$$

where $|CS_i^{(n)}|$ returns the number of items in $CS_i^{(n)}$, namely $|CS_i^{(n)}|$ denotes the number of centric nodes of all items in $CS_i^{(n)}$. m is degree of fuzziness. $d_{y,x}$ denotes the distance between e_y and centric node e_x of S_x; $\sum_{c=1}^{|CS_i^{(n)}|} d_{c,x}$ denotes the total sum of distance between e_y and centric nodes of other items in $CS_i^{(n)}$. The objective function of FCM can be defined as [37]:

$$J = \sum_{i=1}^{|E_i|} \sum_{j=1}^{|CS_i^{(n)}|} M_{i,j} d_{i,j}, \sum_{j=1}^{|CS_i^{(n)}|} M_{i,j} = 1 \tag{13}$$

Let S_r be set of disperse events. J_k^v is defined as value of objective function where k is the number of refinement round; v is the number of re-calculation in the current round. The process of refinement of clusters in $CS_i^{(n)}$ is described, as follows.

Step 1: The cluster S which is not refined in the current refinement round is extracted from $CS_i^{(n)}$. The item which

has the maximum distance with centric node of S is removed from S.

Step 2: Because there is the change of construction of S, the centric node of S needs to be reselected and the value J of objective function needs to be re-calculated (The new value of objective function is marked as J_k^{v+1}). If $J_k^{v+1} < J_k^v$, the removed item from S is considered as a noise event and is added into S_r. S is marked as the refined cluster. If $J_k^{v+1} \geq J_k^v$, the removed item from S cannot be considered as a noise event and is re-added into S. The original centric node of S still acts as centric node of S. S is marked as the unrefined cluster.

Step 3: If there is the unmarked clusters in $CS_i^{(n)}$, the refinement process returns Step 1; Otherwise, implementing Step 4.

Step 4: If all clusters in $CS_i^{(n)}$ are marked and the number of refined clusters is equal or greater than 1, the number of refinement round is marked as $k+1$. The marks of all clusters in $CS_i^{(n)}$ are removed and the refinement process returns to Step 1; Otherwise, implementing Step 5.

Step 5: If all clusters in $CS_i^{(n)}$ are marked as the unrefined clusters, the current refinement iteration is terminated and all clusters in $CS_i^{(n)}$ are considered as refined clusters.

The each cluster in $CS_i^{(n)}$ is considered as one type of encounter events; The centric node of each cluster in $CS_i^{(n)}$ is considered as pattern of the type of encounter events. In other words, the encounter event patterns between n_i and other nodes can be defined as a set EPS_i which includes the centric nodes of all clusters in $CS_i^{(n)}$. Similarly, the encounter event patterns of all nodes in networks can be obtained according to the above method.

E. D2D COMMUNICATIONS BASED ON FAST ENCOUNTER PATTERN RECOGNITION

The time length of encounter and the variation rate of geographical distance are the two characteristic items of encounter events and are used to calculate similarity levels between encounter events. The representation accuracy of encounter event relies on number of gathered characteristic data samples, namely the more the number of samples is, the higher the accuracy of event representation is. The high accuracy of event representation reduces the deviation level of membership degree between encounter events and patterns. However, the number of characteristic data samples is related with the gathered time length. The long gather time leads to the less available time of video data delivery between nodes, which reduces the video sharing efficiency. We design an encounter event recognition strategy, which makes use of small amount of characteristic data samples to accurately calculate membership degree between encounter patterns and events.

In order to ensure efficient sharing of video data, the video request node n_i needs to select an encounter node which stores the requested video and has stable movement state relative to n_i. The stable movement behaviors between n_i and encounter node not only support long-term data transmission with one-hop relationship, but also ensure stability of data transmission rate between them. Let NS_a denote encounter node set of n_i at t_a. We filter noise encounter patterns and noise nodes in NS_a in terms of encounter time length and data transmission rate between n_i and encounter nodes. By estimation of link rate between n_i and all items in NS_a according to the Eq. (2), n_i calculates time length of delivering video v_x between n_i and items in NS_a. If the duration time of an encounter pattern between n_i and an item in NS_a is less than the delivery time between them, the pattern is considered as a noise pattern. If all patterns between a node and n_i are noise, the node can be removed from NS_a.

After removing noise patterns and nodes, n_i select a video provider from NS_a in terms of membership degree of encounter patterns between n_i and items in NS_a. For instance, n_j is an item in NS_a. The encounter event of n_i and n_j is marked as $e_{i,j}^a$. The encounter patterns between n_i and n_j are corresponding to all items in the intersection set $\Omega_{i,j}$ of $CS_i^{(n)}$ and $CS_j^{(n)}$. $e_{i,j}^a$ includes a sample $d_{i,j}(t_a)$ of geographical distance between n_i and n_j at the time t_a of initial encounter of n_i and n_j. $d_{i,j}(t_a)$ is added into the data sets of geographical distance of an item e_k in $\Omega_{i,j}$. e_k recalculates the variation rate b_k of geographical distance. The centric node in the encounter event cluster corresponding to e_k is reselected. If e_k is not selected as the centric node, $e_{i,j}^a$ and e_k are marked as the dissimilar events, which means that $d_{i,j}(t_a)$ is a noise sample for e_k; Otherwise, if e_k is still selected as the centric node, $e_{i,j}^a$ and e_k are marked as the similar events, which means that $d_{i,j}(t_a)$ is a valid sample for e_k. If $e_{i,j}^a$ is similar with e_k, $\sigma_k = \bar{d}_k^{(o)} - \bar{d}_k^{(c)}$ denotes the difference between original and current average distance of e_k and other events in current cluster, namely deviation caused by $d_{i,j}(t_a)$. According to the above process, the distance deviation of events in $\Omega_{i,j}$ which are similar with $e_{i,j}^a$ are calculated. If σ_k is the least deviation value among all distance deviation, e_k is considered as the pattern corresponding to $e_{i,j}^a$. The window length of encounter time of n_i and n_j is defined as:

$$\omega_{i,j} = \frac{l_k}{2^{\alpha_{i,j}}} \tag{14}$$

where l_k is the encounter time length of pattern e_k corresponding to $e_{i,j}^a$; $\alpha_{i,j}$ is the number of variation of pattern corresponding to $e_{i,j}^a$; The initial value of $\alpha_{i,j}$ is 0. Therefore, the initial window length of encounter time of n_i and n_j is $\omega_{i,j} = l_k$ where $\alpha_{i,j} = 0$ and l_k is the encounter time length of e_k. If the pattern corresponding to $e_{i,j}^a$ frequently changes, the window length of encounter time of n_i and n_j fast decreases due to increasing value of $\alpha_{i,j}$, which reduces time of video data sharing between n_i and n_j.

Similarly, the distance deviation values of subjected patterns between n_i and other items in NS_a can be calculated. If an encounter pattern e_k of n_i and a node n_j in NS_a has the least distance deviation among all distance deviation values, e_k becomes the pattern corresponding to $e_{i,j}^a$. The initial window length of encounter time of n_i and n_j is $\omega_{i,j} = l_k, l_k > L_x$

where $\alpha_{i,j} = 0$. At the moment, n_i constructs a connection with n_j and sends a video request message to n_j. After n_j receives the video request message from n_i, n_j delivers the data of video v_x to n_i. After experiencing the second search period t_2, n_i and all items in $NS_a^{(1)}$ generate the new geographical distance samples. n_i makes use of these geographical distance samples to recalculate the new distance deviation values. If e_k still has the least distance deviation, e_k becomes the pattern corresponding to $e_{i,j}^a$ and n_j continues to deliver the data of video v_x to n_i; If an encounter pattern e_x of n_i and an item n_h in NS_a becomes the pattern corresponding to $e_{i,j}^a$, the window length of encounter time of n_i and n_h is the encounter time length $\omega_{i,j} = l_x$ of e_x. n_i sends a video request message containing location information of current playback point to n_h. After n_h receives the request message from n_i, n_h continues to deliver video data to n_i according to the playback point location.

Although n_i disconnects with n_j, the window length of encounter time of n_i and n_j still is redefined as $\omega_{i,j} = \frac{l_k}{2}$ where $\alpha_{i,j} = 1$. If $\frac{l_k}{2} < L_x$, n_j is removed from NS_a and other items in NS_a form a new set $NS_a^{(1)}$; Otherwise, if $\frac{l_k}{2} \geq L_x$, n_j still is included in NS_a. In terms of the above process, after experiencing a new search period, n_i recalculates the distance deviation values based on the new geographical distance samples and fetches the remaining data from the video provider corresponding to the selected encounter pattern. The convergence condition of the above process is n_i has received all data of the requested video or does not search appropriate video providers which do not provide enough encounter time.

The frequent replacement of video provider breaks playback continuity and increases the startup delay. In order to reduce the frequency of replacement of provider caused by the erroneous pattern matching, we add a weight μ for the distance deviation between n_i and other nodes in NS_a. For instance, if e_k has the least distance deviation values σ_k among all encounter patterns of n_i and n_j, the weight $\mu_{i,j}$ corresponding to σ_k is defined as:

$$\mu_{i,j} = \begin{cases} \dfrac{f_t}{f_t - f_r}, & f_t > f_r \\ 0, & f_t \leq f_r \end{cases} \tag{15}$$

where f_t is the total number of encounter of n_i and n_j; f_r denotes the number that e_k being replaced after e_k becomes the pattern corresponding to $e_{i,j}^a$. The more the number of replacement is, the larger the distance deviation value is. In terms of the historical statistical information of pattern replacement, the video requesters can find video providers with stable movement behaviors and reduce the selection probability of video providers with instable movement behaviors. Algorithm 2 describes the search process of video provider of n_i. The complexity of Algorithm 2 is $O(n^2)$ and DMSEM has the same complexity of the algorithm 2 for the search process with the state-of-the-art solutions [25], [38].

Algorithm 2 Search Process of Video Provider

```
/*L_i is length of video data received by n_i; */
n_i searches one-hop D2D communication objects;
communication objects of n_i form a set NS_a;
for(i = 0; i < |NS_a|; i++)
 NS_a[i].Ω is intersection set of patterns between NS_a[i]
 and n_i;
  estimates link rate between NS_a[i] and n_i by eq.(2);
  calculates video delivery time between NS_a[i]
  and n_i;
  for(j = 0; j < |NS_a[i].Ω|; j++)
  if duration l of NS_a[i].Ω[j] is less than delivery time
      NS_a[i].Ω[j] is removed from NS_a[i].Ω;
    end if
  end for
  if Ω == Null
    NS_a[i] is removed from NS_a
  end if
end for
while(L_i < L_x)
  for(i = 0; i < |NS_a|; i++)
    get geographical distance sample set d of NS_a[i]
    and n_i;
    for(j = 0; j < |NS_a[i].Ω|; j++)
      d is added geographical distance set DS of Ω[j];
      calculates variation rate b of Ω[j];
      if Ω[j] is centric node of original event cluster
        calculates deviation σ caused by d;
        σ is added into list DL[i];
      end if
    end for
    σ^j_min is minimum deviation in DL[i];
    σ^j_min is added into list ML;
  end for
  calculates weighted deviation for items in ML by
  eq.(17);
  σ_min is minimum weighted deviation in ML;
  if video provider of n_i is null
    node corresponding to σ_min is provider of n_i;
    sets window length of encounter time by eq.(16);
  else if current provider is not node corresponding
  to σ_min
      replaces current provider;
      resets window length of current and original
      provider;
    end if
  end if
  n_i receives video data from provider;
end while
```

F. PARAMETER SETTINGS

In this section, a series of simulation tests has been conducted to compare the performance of our proposed DMSEM with two state-of-the-art solutions: SV-MAC [19] and UE-NW [20]. In UE-NW, a two stage-based D2D selection

method is proposed: 1) The first stage exploits an intuitionistic fuzzy scheme to estimate the social and preference similarity; 2) The second stage selects the D2D partners by solving an integer linear programming problem. In SV-MAC, a social-aware D2D connection discovery is presented, which controls the D2D links via a social graph resided in each user equipment's repository.

The simulation time is set to 500 s. The simulation scenario is a 2000 $\times$ 2000 m^2 square with 200 mobile nodes moving according to the random way point model [39]. The enough large scenario can support the simulation of relatively real movement behaviors of mobile nodes and collect the complete and various movement traces of mobile nodes. In this mobility model, each node first chooses the destination within the area following the uniform distribution. Then, it randomly selects a velocity and begins to move. After reaching the destination, the node repeats the above process and continue moving. The velocity ranges from [10, 40] m/s, unless otherwise specified. 25 base stations uniformly are distributed in the scenarios and act as the AP to support the mobile nodes accessing to the video content. The 5G D2D setting follows the settings of the 5G D2D simulation in the popular current studies [40].

To approximate the real scenarios, there are 40 different videos shared among the mobile nodes. These videos are segmented and each segments is 2 s long with the size ranging from 100 KB - 500 KB, The time length of each video ranges from 120 s to 240 s. Mobile nodes request the videos by the Zipf distribution, which means for the 40 videos, the probability of requesting the n-th popular video can be given by [41]

$$P(n) = \frac{\sum_{k=1}^{40} \frac{1}{k^{\rho}}}{r^{\rho}} \tag{16}$$

where ρ is the Zipf constant and is set to 0.8. Each user generates video request message following the Poission distribution with 0.1. For each mobile node, the LRU caching replacement scheme is applied.

For the D2D communication, we utilize the 802.11p as the MAC proctocl and set the upper bound of data rate to 27 $Mbps$. The maximum communication range is 250 m and the MAC channel delay is 250 ms. The propagation loss model is the Friis Propagation Loss Model (FPLM) in NS3 [42]. The FPLM is designed for unstructured clear path between receiver and transmitter, which eliminates the performance degraded by random shadowing effects. Therefore, the simulation tests derived by using FPLM can be more for convincible since the results erase the random effects caused by shadowing.

G. PERFORMANCE EVALUATION

The performance of DMSEM is compared with that of SV-MAC and UE-NW in terms of packet loss rate (PLR), average freeze time, average bitrate, buffer level and control overhead, respectively.

(1) Average packet loss rate (APLR): We define APLR as the ratio between the number of received packets and the number of sent packets. Fig. 4 shows how the APLR values of three solutions vary with increasing simulation time. The three curves corresponding to the the three solutions experience a decreasing trend before the 300 s and then remain stable. The reason for the decrement is that the accuracy of choosing D2D clusters increases over the time, as more and more users' moving pattern or social relationships are captured by the D2D discovery schemes. After 100 s, the three curves corresponding to the three solutions have a stable phase since the arrival and departure of viewers is balanced. DMSEM outperforms the other two solutions, i.e., DMSEM is about 15% (17%, respectively) lower than the SV-MAC (UE-NW, respectively) when in stable phase.

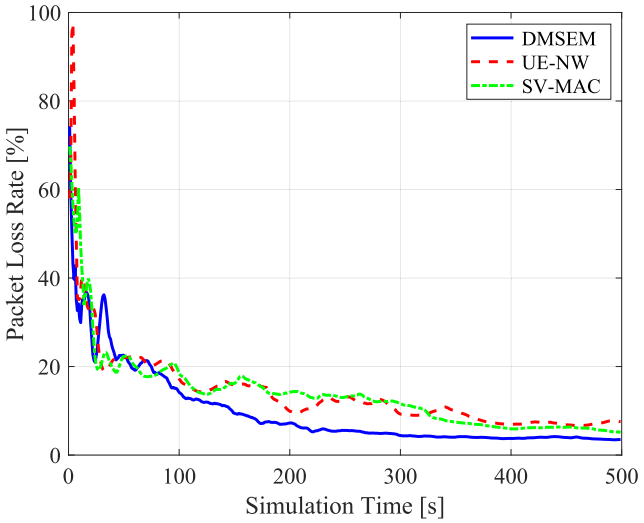

FIGURE 4. Average packet loss rate against simulation time.

Fig. 5 shows the APLR of three solutions under different velocity ranges. All bars corresponding to the three solutions rises with increasing velocity. This is mainly because fast speed may shorten the encounter time of mobile nodes and also raise the risk of long distance transmission. Accessing the video from remote providers increases the packet loss probability due to the complex channel condition. Also, the short encounter time also results in the frequent interruption of content delivery. Comparing with SV-MAC and UE-NW, DMSEM achieves a much lower APLR. Especially, the APLR of DMSEM is below the 15% during the simulation and other twos are around 17%.

The two social-based solutions have similar performance, since they mainly rely on the similarity of social relationship to discover the D2D connection. The superiority of DMSEM is because it provides more accurate D2D provider selection. Unlike the two social-based solutions search the D2D pairs by the social relationships, DMSEM extracts the encounter patterns by clustering the encounter events. Especially, a rapid pattern recognition algorithm is proposed which achieves the fast convergence while ensures the accuracy. Thus, comparing with other two solutions, DMSEM has the better performance on selecting the video providers with low distance and stable link states, which achieves a lower

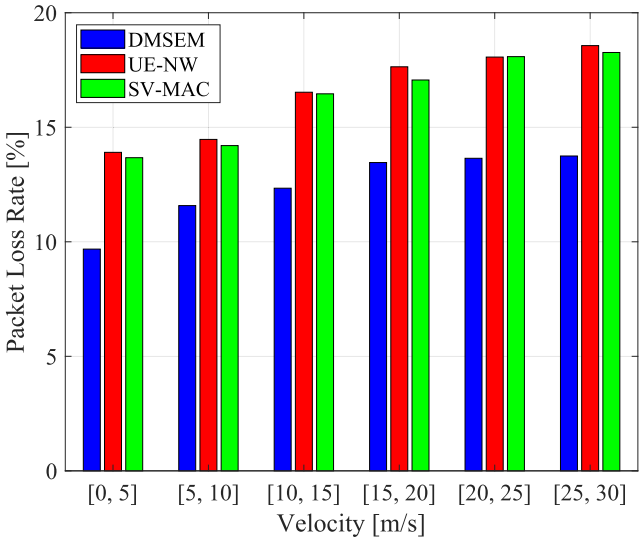

FIGURE 5. Average packet loss rate against velocity.

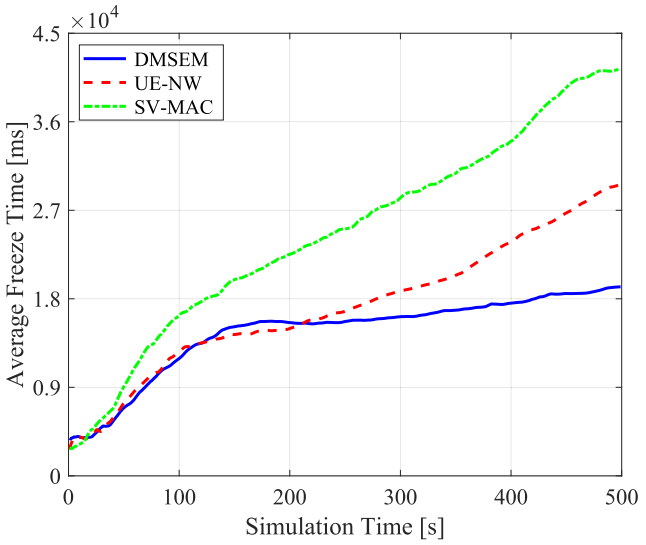

FIGURE 6. Average freeze time against simulation time.

bitrate loss. Besides, DMSEM also achieves a lower PLR because the encounter patterns are considered. Accurate the awareness and recognition of encounter patterns ensure the most of devices can maintain a stable delivery link. Therefore, the single consideration for the social relationship difficultly ensures the long-term stability between mobile devices since the movement behaviors are random in most cases.

(2) Average freeze time (AFT): The average freeze time is defined as [43]:

$$AFT = \frac{\sum_{v=1}^{V} f_v}{V} \tag{17}$$

where V denotes the overall playback times of video during the simulation time; f_v is the freeze time of v^{th} playing video. Fig 6 plots the variation of three solutions' AFT with increasing simulation time. The three curves reveal an increasing trend given the fact that the network is becoming crowded with more and more users requesting the video. The increasing occurrence of concurrent video delivery rises the average video access latency and thereby enlarging the AFT. DMSEM achieves the lowest AFT after 220 s, which ranges from 1.6 s to 1.8 s. The UE-NW has the better performance than that of SV-MAC, i.e., UE-NW and SV-MAC AFT are 2.9 and 4.3 at 500 s, respectively. Fig 7 shows the AFT under different speed range. We observe that the values of all solutions' AFT keep rise trend with increasing velocity. This is mainly because that the a higher speed may result in a higher probability of delivery interruption. Similarly as Fig. 6, DMSEM outperforms the other two solutions in terms of AFT and advantages expands in higher moving speed.

The reasons for DMSEM having the lowest AFT can be explained: DMSEM accurately clusters the encounter events between mobile users to accurately extract the encounter patterns and fast recognize the encounter patterns of mobile users. Hence, DMSEM provides more stable D2D link and also shortens the delivery latency. SV-MAC and UE-NW

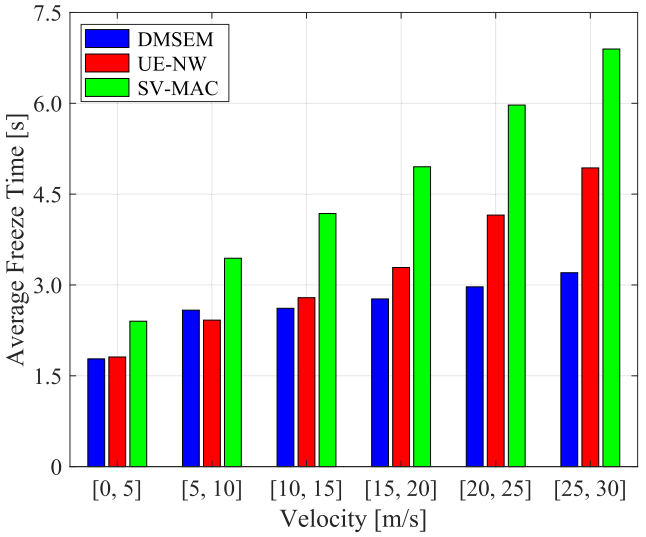

FIGURE 7. Average freeze time against velocity.

only consider the social relationship, so that they suffers unstable D2D communications due to short encounter time between two D2D partners. UE-NW solution is better than that of SV-MAC since it considers not only the social relationship, but also the viewers preferences. The mobile users with similar preferences may have identical demand on video content, which increases the probability of discovering the D2D links.

(3) Average bitrate (AB). As Fig.8 the results of AB confirm that DMSEM achieves the best performance on content delivery. The reasons are two-folded: (1) DMSEM stabilizes the D2D communications via capturing the encounter patterns of mobile nodes and selects the D2D partners with high similar encounter patterns, which stabilizes the D2D links during the whole transmission process. The stable link ensures the smooth delivery which reduces the packet loss

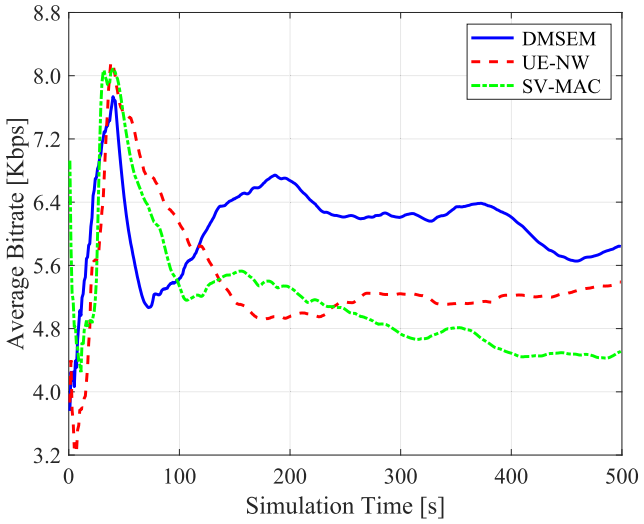

FIGURE 8. Average bitrate against simulation time.

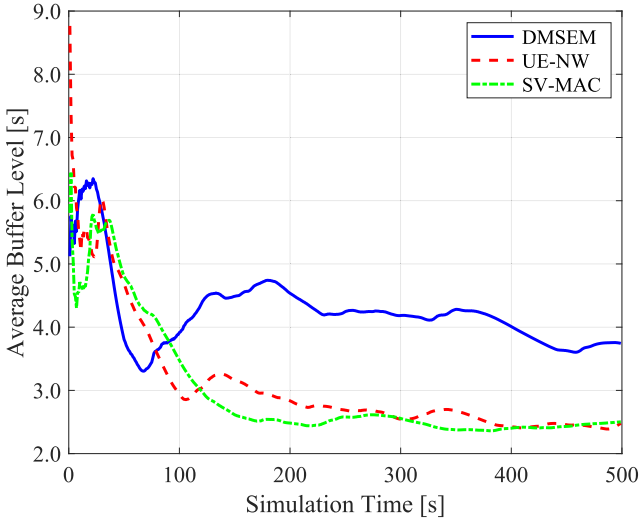

FIGURE 9. Buffer level against simulation time.

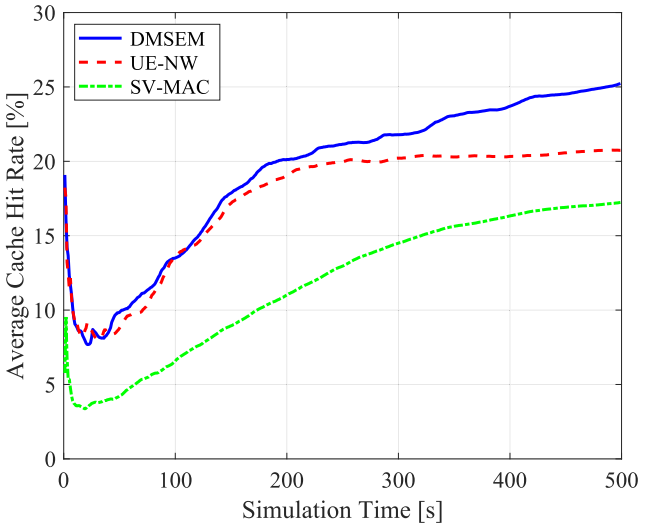

FIGURE 10. Average cache hit ratio against simulation time.

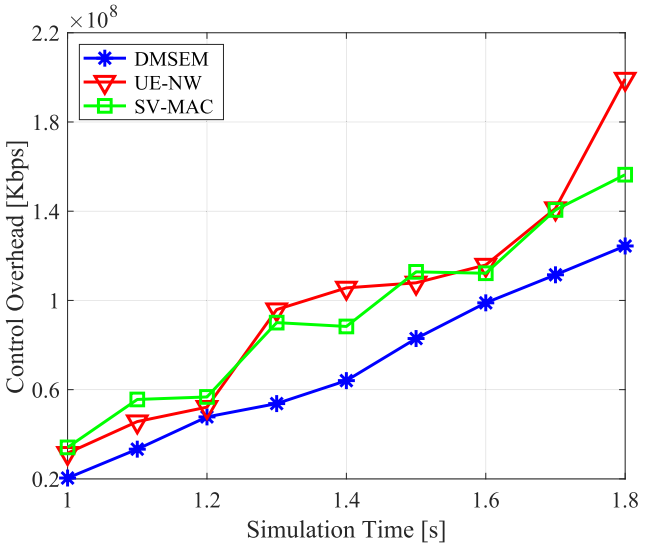

FIGURE 11. Control overhead against simulation time.

and occurrence of interrupt; (2) DMSEM also selects the pairing nodes with shorter distance to access the content, which can also improve the channel conditions, thereby increasing the data rate given the better channel state.

The results of AB confirm that DMSEM achieves the best performances on content delivery. The reasons are explained by the following two-folded: (1) the stable link ensures the smooth delivery which reduces the packet loss and occurrence of interrupt; (2) Accessing content with nearby nodes also improves the data rate given the better channel state.

(4) Buffer Level (BL): Fig. 9 shows the average buffer level of users of three solutions during the whole simulation time. By comparing with UE-NW and SV-MAC, DMSEM has the highest buffer level, i.e., 4.5 *s*, 2.8 *s* and 2.5 *s* for DMSEM, UE-NW and SV-MAC at 200 *s*, respectively. The results confirm that DMSEM has the lowest BL values since for the most of mobile users and the video contents in buffer are enough for the smooth playback.

(5) Average Cache hit ratio (ACHR): This parameter is calculated by the ratio between total number of sent request messages and number of satisfied requests. Fig. 10 shows that DMSEM achieves the highest ACHR. Namely, the more users can access the video content within one-hop range when using DMSEM. By comparing with the social-based solutions UE-NW and SV-MAC, the accurate and fast recognition for the encounter patterns can provide more accurate D2D connection discovery. UE-NW performance is better than that of SV-MAC. This is because UE-NW considers not only users mobility but also the preference selection. The requested content is more likely cached by the nodes with similar preference. Thus, UE-NW achieves better cache hit ratio than SV-MAC.

(6) Control Overhead (CO): Figure 11 shows the CO caused by deploying the three D2D delivery schemes. The three curves corresponding to the three solutions

experience a rise trend because of the increase in the number of video requesters. DMSEM has lower CO since it only requires video sharing between mobile nodes with the similar encounter patterns. In fact, DMSEM makes use of the complex computation of similar encounter patterns to compensate the control overhead of D2D communication pairing. Unlike DMSEM, UE-NW and SV-MAC discover the D2D connections by estimating the social relationships, which requires the mobile devices continuously collect the information about social interactions for estimating the social similarity between mobile users, which may consume much communication resources.

IV. CONCLUSION AND OPEN RESEARCH ISSUES

In this paper, we propose a novel Social-Aware D2D Video Delivery Method based on Rapid Sample-Efficient Measurement of Mobility Similarity in 5G Ultra-Dense Network (DMSEM). DMSEM makes use of social state transition to describe encounter event samples of fitting one-hop D2D video sharing in terms of one-hop D2D pair relationship and comparison between encounter duration and shared video length. By expression of encounter events using variation rate of geographical distance between mobile users and encounter duration time and implementing iterative search and mergence in graph according to distance between events and centrality gain of mergence, the initial clusters of encounter events are generated. DMSEM makes use of the Fuzzy C-Means (FCM) to remove noises in initial event cluster and refine accuracy levels of initial clustering, to extract encounter patterns of mobile users. DMSEM employs a sample-efficiency rapid recognition algorithm of encounter pattern to achieve fast heuristic recognition of encounter pattern. DMSEM achieves better results in comparison with other state-of-the-art solutions SV-MAC and UE-NW in terms of packet loss rate, average freeze time, cache utilization, average bitrate, buffer level and control overhead. We investigate the mobility management to enhance the performance of D2D communications in the future.

REFERENCES

[1] C. Ge, N. Wang, I. Selinis, J. Cahill, M. Kavanagh, K. Liolis, C. Politis, J. Nunes, B. Evans, Y. Rahulan, N. Nouvel, M. Boutin, J. Desmauts, F. Arnal, S. Watts, and G. Poziopoulou, "QoE-assured live streaming via satellite Backhaul in 5G networks," *IEEE Trans. Broadcast.*, vol. 65, no. 2, pp. 381–391, Jun. 2019.

[2] N.-S. Vo, T. Q. Duong, H. D. Tuan, and A. Kortun, "Optimal video streaming in dense 5G networks with D2D communications," *IEEE Access*, vol. 6, pp. 209–223, 2018.

[3] T. Huang, W. Yang, J. Wu, J. Ma, X. Zhang, and D. Zhang, "A survey on green 6G network: Architecture and technologies," *IEEE Access*, vol. 7, pp. 175758–175768, 2019.

[4] M. Wang, C. Xu, X. Chen, H. Hao, L. Zhong, and D. O. Wu, "Design of multipath transmission control for information-centric Internet of Things: A distributed stochastic optimization framework," *IEEE Internet Things J.*, vol. 6, no. 6, pp. 9475–9488, Dec. 2019.

[5] Z. Jiang, C. Xu, J. Guan, Y. Liu, and G.-M. Muntean, "Stochastic analysis of DASH-based video service in high-speed railway networks," *IEEE Trans. Multimedia*, vol. 21, no. 6, pp. 1577–1592, Jun. 2019.

[6] G. S. Park and H. Song, "Video quality-aware traffic offloading system for video streaming services over 5G networks with dual connectivity," *IEEE Trans. Veh. Technol.*, vol. 68, no. 6, pp. 5928–5943, Jun. 2019.

[7] S. Song, J. Jung, M. Choi, C. Lee, J. Sun, and J.-M. Chung, "Multipath based adaptive concurrent transfer for real-time video streaming over 5G multi-RAT systems," *IEEE Access*, vol. 7, pp. 146470–146479, 2019.

[8] J. Nightingale, P. Salva-Garcia, J. M. A. Calero, and Q. Wang, "5G-QoE: QoE modelling for ultra-HD video streaming in 5G networks," *IEEE Trans. Broadcast.*, vol. 64, no. 2, pp. 621–634, Jun. 2018.

[9] M. Jaber, M. A. Imran, R. Tafazolli, and A. Tukmanov, "5G backhaul challenges and emerging research directions: A survey," *IEEE Access*, vol. 4, pp. 1743–1766, 2016.

[10] M. Shafi, A. F. Molisch, P. J. Smith, T. Haustein, P. Zhu, P. De Silva, F. Tufvesson, A. Benjebbour, and G. Wunder, "5G: A tutorial overview of standards, trials, challenges, deployment, and practice," *IEEE J. Sel. Areas Commun.*, vol. 35, no. 6, pp. 1201–1221, Jun. 2017.

[11] D. Wu, J. Wang, R. Q. Hu, Y. Cai, and L. Zhou, "Energy-efficient resource sharing for mobile device-to-device multimedia communications," *IEEE Trans. Veh. Technol.*, vol. 63, no. 5, pp. 2093–2103, Jun. 2014.

[12] C. Xu, M. Wang, X. Chen, L. Zhong, and L. A. Grieco, "Optimal information centric caching in 5G device-to-device communications," *IEEE Trans. Mobile Comput.*, vol. 17, no. 9, pp. 2114–2126, Sep. 2018.

[13] A. Zhang, J. Chen, L. Zhou, and S. Yu, "Graph theory-based QoE-driven cooperation stimulation for content dissemination in device-to-device communication," *IEEE Trans. Emerg. Topics Comput.*, vol. 4, no. 4, pp. 556–567, Oct. 2016.

[14] L. Zhou, D. Wu, J. Chen, and Z. Dong, "Greening the smart cities: Energy-efficient massive content delivery via D2D communications," *IEEE Trans Ind. Informat.*, vol. 14, no. 4, pp. 1626–1634, Apr. 2018.

[15] M. Wang, C. Xu, X. Chen, H. Hao, L. Zhong, and S. Yu, "Differential privacy oriented distributed online learning for mobile social video prefetching," *IEEE Trans. Multimedia*, vol. 21, no. 3, pp. 636–651, Mar. 2019.

[16] D. Wu, L. Zhou, Y. Cai, H.-C. Chao, and Y. Qian, "Physical–social-aware D2D content sharing networks: A provider–demander matching game," *IEEE Trans. Veh. Technol.*, vol. 67, no. 8, pp. 7538–7549, Aug. 2018.

[17] D. Wu, L. Zhou, Y. Cai, and Y. Qian, "Optimal content sharing mode selection for social-aware D2D communications," *IEEE Wireless Commun. Lett.*, vol. 7, no. 6, pp. 910–913, Dec. 2018.

[18] D. Wu, L. Zhou, and Y. Cai, "Social-aware rate based content sharing mode selection for D2D content sharing scenarios," *IEEE Trans. Multimedia*, vol. 19, no. 11, pp. 2571–2582, Nov. 2017.

[19] B. Fan, H. Tian, L. Jiang, and A. V. Vasilakos, "A social-aware virtual MAC protocol for energy-efficient D2D communications underlying heterogeneous cellular networks," *IEEE Trans. Veh. Technol.*, vol. 67, no. 9, pp. 8372–8385, Sep. 2018.

[20] K. Wu, M. Jiang, and H.-Z. Tan, "D2D relay selection based on joint fuzzy and entropy theories with social similarity," *IEEE Trans. Veh. Technol.*, vol. 67, no. 9, pp. 8796–8807, Sep. 2018.

[21] Z. Wang, L. Sun, M. Zhang, H. Pang, E. Tian, and W. Zhu, "Propagation- and mobility-aware D2D social content replication," *IEEE Trans. Mobile Comput.*, vol. 16, no. 4, pp. 1107–1120, Apr. 2017.

[22] B. Ying and A. Nayak, "A power-efficient and social-aware relay selection method for multi-hop D2D communications," *IEEE Commun. Lett.*, vol. 22, no. 7, pp. 1450–1453, Jul. 2018.

[23] Y. Li, S. Su, and S. Chen, "Social-aware resource allocation for device-to-device communications underlaying cellular networks," *IEEE Wireless Commun. Lett.*, vol. 4, no. 3, pp. 293–296, Jun. 2015.

[24] B. Zhang, Y. Li, D. Jin, P. Hui, and Z. Han, "Social-aware peer discovery for D2D communications underlaying cellular networks," *IEEE Trans. Wireless Commun.*, vol. 14, no. 5, pp. 2426–2439, May 2015.

[25] X. Chen, B. Proulx, X. Gong, and J. Zhang, "Exploiting social ties for cooperative D2D communications: A mobile social networking case," *IEEE/ACM Trans. Netw.*, vol. 23, no. 5, pp. 1471–1484, Oct. 2015.

[26] X. Chen, Y. Zhao, Y. Li, X. Chen, N. Ge, and S. Chen, "Social trust aided D2D communications: Performance bound and implementation mechanism," *IEEE J. Sel. Areas Commun.*, vol. 36, no. 7, pp. 1593–1608, Jul. 2018.

[27] J. Yoon, B. D. Noble, M. Liu, and M. Kim, "Building realistic mobility models from coarse-grained traces," in *Proc. 4th Int. Conf. Mobile Syst., Appl. Services (MobiSys)*, Jun. 2006, pp. 177–190.

[28] M. Waqas, Y. Niu, Y. Li, M. Ahmed, D. Jin, S. Chen, and Z. Han, "Mobility-aware device-to-device communications: Principles, practice and challenges," *IEEE Commun. Surveys Tuts.*, to be published.

[29] W.-D. Wu, C.-C. Lee, C.-H. Wang, and C.-C. Chao, "Signal-to-interference-plus-noise ratio analysis for direct-sequence ultra-wideband systems in generalized Saleh–Valenzuela channels," *IEEE J. Sel. Topics Signal Process.*, vol. 1, no. 3, pp. 483–497, Oct. 2007.
[30] A. V. Makkuva and Y. Wu, "Equivalence of additive-combinatorial linear inequalities for Shannon entropy and differential entropy," *IEEE Trans. Inf. Theory*, vol. 64, no. 5, pp. 3579–3589, May 2018.
[31] G. Mateos, J. A. Bazerque, and G. B. Giannakis, "Distributed sparse linear regression," *IEEE Trans. Signal Process.*, vol. 58, no. 10, pp. 5262–5276, Oct. 2010.
[32] S. Jia, C. Xu, J. Guan, H. Zhang, and G.-M. Muntean, "A novel cooperative content fetching-based strategy to increase the quality of video delivery to mobile users in wireless networks," *IEEE Trans. Broadcast.*, vol. 60, no. 2, pp. 370–384, Jun. 2014.
[33] B. Yang and C. A. Balanis, "Least square method to optimize the coefficients of complex finite-difference space stencils," *IEEE Antennas Wireless Propag. Lett.*, vol. 5, pp. 450–453, Oct. 2006.
[34] S. A. Rizvi and N. M. Nasrabadi, "An efficient Euclidean distance computation for vector quantization using a truncated look-up table," *IEEE Trans. Circuits Syst. Video Technol.*, vol. 5, no. 4, pp. 370–371, Aug. 1995.
[35] S. Segarra and A. Ribeiro, "Stability and continuity of centrality measures in weighted graphs," *IEEE Trans. Signal Process.*, vol. 64, no. 3, pp. 543–555, Feb. 2016.
[36] O. Linda and M. Manic, "General type-2 fuzzy C-means algorithm for uncertain fuzzy clustering," *IEEE Trans. Fuzzy Syst.*, vol. 20, no. 5, pp. 883–897, Oct. 2012.
[37] C. Xu, S. Jia, M. Wang, L. Zhong, H. Zhang, and G.-M. Muntean, "Performance-aware mobile community-based VoD streaming over vehicular ad hoc networks," *IEEE Trans. Veh. Technol.*, vol. 64, no. 3, pp. 1201–1217, Mar. 2015.
[38] D. Singh and S. C. Ghosh, "Mobility-aware relay selection in 5G D2D communication using stochastic model," *IEEE Trans. Veh. Technol.*, vol. 68, no. 3, pp. 2837–2849, Mar. 2019.
[39] R. Groenevelt, P. Nain, and G. Koole, "The message delay in mobile ad hoc networks," *Perform. Eval.*, vol. 62, nos. 1–4, pp. 210–228, Oct. 2005.
[40] H. Zhang, Y. Liao, and L. Song, "D2D-U: Device-to-device communications in unlicensed bands for 5G system," *IEEE Trans. Wireless Commun.*, vol. 16, no. 6, pp. 3507–3519, Jun. 2017.
[41] Q. Li, Y. Zhang, A. Pandharipande, X. Ge, and J. Zhang, "D2D-assisted caching on truncated Zipf distribution," *IEEE Access*, vol. 7, pp. 13411–13421, 2019.
[42] A. Aldalbahi, M. Rahaim, A. Khreishah, M. Ayyash, and T. D. C. Little, "Visible light communication module: An open source extension to the ns3 network simulator with real system validation," *IEEE Access*, vol. 5, pp. 22144–22158, 2017.
[43] S. D. Peters and M. M. Fahmy, "Synthesis of recursive LTV digital filters using the frozen-time approximation," *IEEE Trans. Circuits Syst.*, vol. 36, no. 3, pp. 448–451, Mar. 1989.

RUILING ZHANG received the M.S. degree from Northwestern Polytechnical University, Xi'an, China, in 2007. She is currently a Professor with Luoyang Normal University. Her research interests include intelligent information processing, data mining, and rough set.

SHIJIE JIA (Member, IEEE) received the Ph.D. degree in communications and information system from BUPT, in March 2014. He is currently an Associate Professor with the Academy of Information Technology, Luoyang Normal University, Henan, China. His research interests include next generation Internet technology, wireless communications, and peer-to-peer networks.

YOUZHONG MA received the Ph.D. degree in computer software and theory from the Renmin University of China, in June 2014. He is currently an Associate Professor with the Academy of Information Technology, Luoyang Normal University, Henan, China. His research interests include big data management and analysis, and Web data integration.

CHANGQIAO XU (Senior Member, IEEE) received the Ph.D. degree from the Institute of Software, Chinese Academy of Sciences, Beijing, China, in 2009.

He is currently a Professor with the State Key Laboratory of Networking and Switching Technology, Beijing University of Posts and Telecommunications, Beijing. He has published over 100 technical articles. His current research interests include wireless networking, network transmission control, and next generation Internet. Prof. Xu has served as the Co-Chair for the IEEE MMTC Interest Group, Green Multimedia Communications.